Journal of Machine Engineering, 2026, Vol. 26
ISSN 1895-7595 (Print) ISSN 2391-8071 (Online)

Received*: 13 April 2026* / Accepted: *18 May 2026* / Published online: *02 June 2026*

robotic deburring,
sheet metal finishing,
machine vision,
robotic brushing

Kristo VAHER[1*],
Nikita PIKKAS[1]

AUTOMATED ROBOTIC DEBURRING SYSTEM FOR LASER-CUT SHEET METAL USING MACHINE VISION

Automating the deburring of laser-cut sheet metal parts remains challenging due to the need for both reliable part detection and controlled material removal. This paper presents the development and experimental validation of a vision-guided robotic grinding system for automated deburring of laser-cut metal components. The system integrates a collaborative robot, a custom grinding end-effector, a load-cell-based force control system, and a machine vision setup using optimized backlighting and contour detection. Qualitative results showed complete burr, dross, and heat-affected zone removal in a single pass for both mild steel and stainless-steel specimens. Reliability testing yielded a 96% success rate across 50 processed parts. The results confirm that integrated machine vision and force-controlled robotic grinding can provide a viable alternative to manual deburring and expensive big machines in sheet metal manufacturing, offering improved consistency, lower physical workload, and competitive processing time.

1. INTRODUCTION

Deburring remains an essential but insufficiently automated finishing process in manufacturing. Burrs, slag, and sharp edges generated during machining or laser cutting can reduce product quality, compromise safety, and interfere with assembly, making post-processing necessary even in otherwise highly automated production chains. In the case of laser-cut sheet metal parts, deburring is still often performed manually, resulting in labour-intensive work, inconsistent quality, and limited scalability.

Automating deburring is challenging because it requires solving two tightly coupled problems: reliable part perception and controlled physical interaction. A robotic system must first detect and localize parts with varying geometries and reflective metal surfaces and then remove defects using a tool that maintains sufficient contact force without causing over-deburring or dimensional inaccuracies. Although previous studies have explored force-

[1] Institute of Technology, TTK University of Applied Sciences, Tallinn, Estonia
[*] E-mail: kristo.vaher@tktk.ee
https://doi.org/10.36897/jme/221958

controlled robotic deburring and vision-assisted contour following, fewer works have addressed their integration in the context of adaptive finishing of laser-cut sheet metal parts.

This paper presents an integrated robotic deburring system that combines machine vision with force-controlled brushing. The system uses a collaborative robot, a custom brushing end-effector, and a backlighting-based contour detection method to localize parts and perform automated edge finishing. The objective of the study is to evaluate whether such a system can achieve the accuracy, consistency, and reliability required to reduce or replace manual deburring in industrial settings. Experimental evaluation focuses on detection accuracy, deburring quality, dimensional control, repeatability, and overall process performance.

2. SELECTION OF DEBURRING METHODS FOR ROBOTIC FINISHING

The transition from manual to robotic deburring is driven by the need for improved repeatability, lower labor dependence, better ergonomics, and safer working conditions in manufacturing environments. Robotic deburring has been identified as a promising enabler of smart manufacturing, particularly in sectors where precision and consistency are critical, such as automotive, aerospace, electronics, and medical devices [1, 2, 3]. However, despite these advantages, deburring remains more difficult to automate than many other industrial operations because it combines two challenging requirements: reliable part localization and controlled physical interaction between tool and workpiece. This is particularly important in the finishing of laser-cut sheet metal, where edge defects such as burrs, dross, striations, kerf taper, oxidation, and micro-spatter often require post-processing even when the cutting stage itself is highly automated [4, 5].

The literature shows that deburring technologies differ significantly in terms of operating principle, surface quality, throughput, cost, and automation suitability. Conventional manual methods remain attractive for prototypes, repair work, and geometrically complex one-off parts because of their flexibility, but they are labor-intensive, inconsistent, and poorly scalable [6, 14, 15]. Automated and machine-based methods, by contrast, provide greater repeatability and production throughput, but typically require higher initial investment and are less adaptable to unusual shapes or small batches. For robot-assisted or robot-arm-based finishing, the most suitable methods identified in the review are contact-based edge finishing processes and robotically guided non-contact processes. In particular, sanding with hand-tool equivalents, hand filing–type finishing, manual polishing/wiping, rotary brush deburring, and water jet deburring are considered the most realistic candidates for robotic implementation. Rotary brush deburring is especially attractive because it is already established in CNC-controlled finishing systems and can be integrated into inline automation. Brush-based finishing is further supported by [7], who showed that stable brush deburring requires controlled contact pressure and benefits from integrated sensing for monitoring tool engagement and wear [16].

Other deburring technologies can be considered robot-compatible only in a broader sense of automation rather than as direct robot-arm end-effector processes. Laser-based

deburring is attractive because of its potential integration with laser cutting lines, but it is more naturally suited to CNC or gantry-type systems than to a deburring robot cell. Electrochemical deburring and plasma electrolytic polishing are highly effective and programmable, but they are process-cell technologies rather than flexible robotic edge-following operations. Thermal deburring is a fast batch method for difficult-to-access burrs, yet it is chamber-based and unsuitable for direct robot-arm interaction. Vibratory finishing or tumbling can also be partly robotized, although in practice the robot is more relevant for loading and unloading than for the deburring action itself. In contrast, abrasive belt grinding is effective and productive for flat parts, but it is generally better suited to conveyor-based machine systems than to flexible robot arms, especially when part geometries vary.

A qualitative cost–performance comparison in the review further supports the selection of robot-compatible methods. Manual processes offer low implementation cost but relatively low process consistency and scalability, whereas advanced automated methods generally achieve higher performance at the cost of greater system complexity, infrastructure requirements, and investment. For robotic finishing, the most balanced methods are those that combine acceptable implementation cost with controllable and repeatable tool–workpiece interaction. This makes brush-based and sanding-based processes particularly attractive for robotic deburring of sheet metal edges, where localized finishing and moderate compliance are required.

The main bottlenecks identified in the literature are directly relevant to the design of robotic deburring systems. First, complex geometry remains a major challenge, since freeform or highly variable part contours often require custom path planning, fixtures, or machine vision support. Second, force feedback limitations are significant because burr size, hardness, and position may vary from part to part, making force-torque sensing and adaptive control essential [8, 9, 10]. Third, part detection and alignment are critical issues, particularly for reflective or irregularly positioned sheet metal parts; without appropriate fixtures or 2D/3D vision systems, robotic localization errors may compromise finishing quality [11, 12, 13]. Fourth, cognitive decision-making remains difficult to automate, as human operators can visually interpret unexpected defects and adapt their actions in ways that robots currently require additional sensing or AI support to reproduce. The review also identifies broader technological bottlenecks, including machine vision sensitivity to reflections and contamination, the lack of standardized compliant end-effectors for fine finishing, and the complexity of integrating vision, force sensing, and motion control into a stable closed-loop system.

Overall, the literature review indicates that the most promising deburring methods for robot-arm-based finishing of laser-cut sheet metal are sanding-based, brush-based, and selected jet-based processes, because these methods can be adapted to localized contour following and benefit directly from force-sensitive control. At the same time, the review makes clear that successful robotic deburring depends not only on method selection, but also on solving the coupled problems of reliable part perception and compliant process control. These findings provide the rationale for the present work, which focuses on integrating machine vision with force-controlled robotic brushing for adaptive finishing of laser-cut sheet metal parts. Based on the literature review, the brush-based deburring method was selected for experimental validation.

3. METHODOLOGY

This study employed an integrated experimental system combining machine vision, robot calibration, and force-controlled brushing to automate the deburring of laser-cut sheet metal parts. The methodology was developed to address the two key challenges identified in the literature: reliable localization of reflective sheet metal parts and stable tool–workpiece interaction during brushing. The proposed approach combines a collaborative robot, a custom end-effector, a vision-guided contour detection pipeline, and a closed-loop force control strategy. The following subsection summarizes the experimental setup and the main processing stages used for system validation.

3.1. EXPERIMENTAL SETUP AND SYSTEM ARCHITECTURE

The experimental system consisted of five integrated subsystems: a Universal Robots UR10 collaborative robot, a custom brushing end-effector, an Intel RealSense D455 vision system, a custom backlit inspection table, and a Raspberry Pi–based control unit. The robot was equipped with a 500 W brushless spindle running at 12,000 rpm and a 25 mm cylindrical abrasive brush selected as the deburring tool. A custom mounting assembly integrated the spindle, dust extraction, camera holder, and an external load cell with approximately 100 N capacity for force feedback, as shown in Fig. 1. This external sensing solution was adopted to enable reliable closed-loop brushing control.

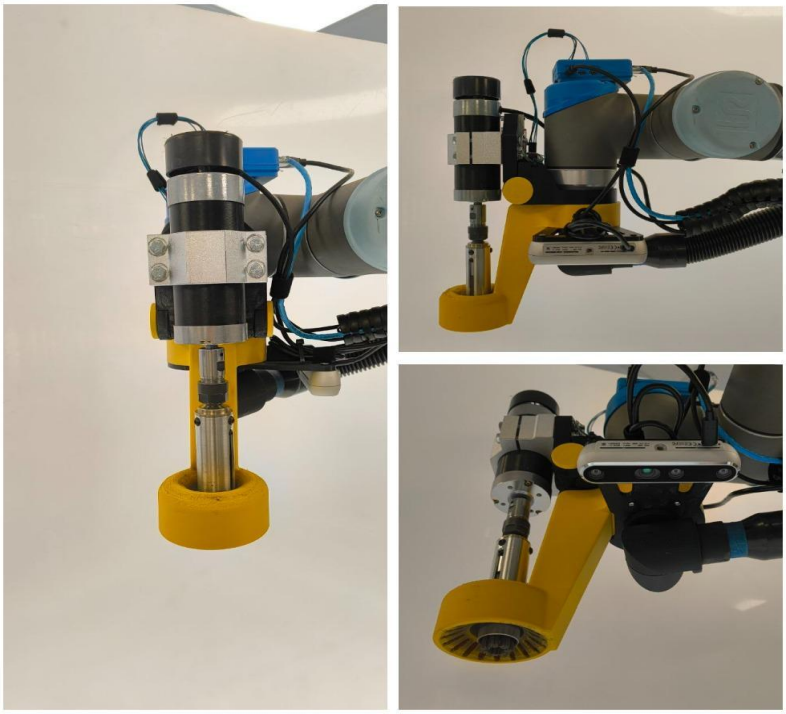

Fig. 1. Photo of UR10 robot with mounted end-effector

To ensure robust visual localization of laser-cut parts, a custom inspection table was developed using an 8 mm white translucent plastic plate. The table acted as a light diffuser and produced a high-contrast silhouette of the workpieces against the background. The final table design is shown in Fig. 2.

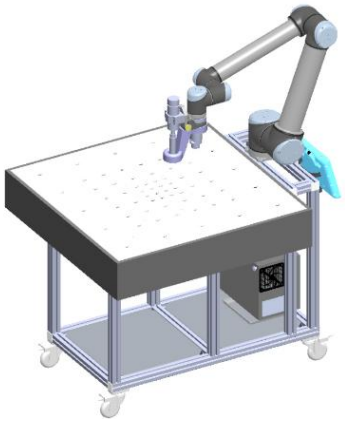

Fig. 2. 3D model of table design

The vision subsystem used an Intel RealSense D455 camera mounted above the table, while the backlighting system employed an LED strip below the translucent surface as illustrated in Fig. 3. The optimal backlight position was selected through comparative experiments in which LED strip and ringlight configurations were tested at heights of 4, 11, 18, and 25 cm under different ambient lighting conditions. The evaluation criteria were contour contrast, illumination homogeneity across the 1 m × 1 m table, and robustness to room-light variation. Among the tested configurations, the LED strip positioned 18 cm below the translucent table surface provided the best compromise between uniform illumination and contour visibility and was therefore selected for the final system configuration. Although the comparison was not expressed through a single numerical optimization metric, the configuration was selected based on repeatable experimental comparison using clearly defined visual-performance criteria.

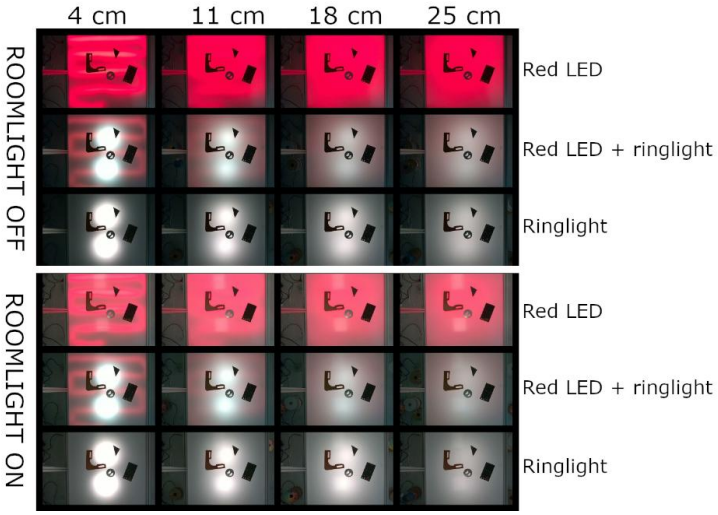

Fig. 3. Systematic comparison of LED strip backlight vs. ring light at different heights (4 cm, 11 cm, 18 cm, 25 cm) with room lighting ON and OFF)

The software architecture combined image acquisition, image processing, load cell data acquisition, and robot communication. A dual-exposure reflectance-ratio method was implemented to detect reflective sheet metal parts on the white table surface. Two images were acquired sequentially: one with the backlight turned off and one with the backlight turned on. Their normalized intensity difference was then used to separate the workpiece from the background despite changes in ambient light. The image processing pipeline included Gaussian filtering, threshold-based segmentation, morphological operations, and hierarchical contour extraction to identify both external contours and internal features. Permanent table features and contamination-related false detections were reduced through a background elimination strategy based on reference images of the empty table. The main image-processing stages are shown in Fig. 4.

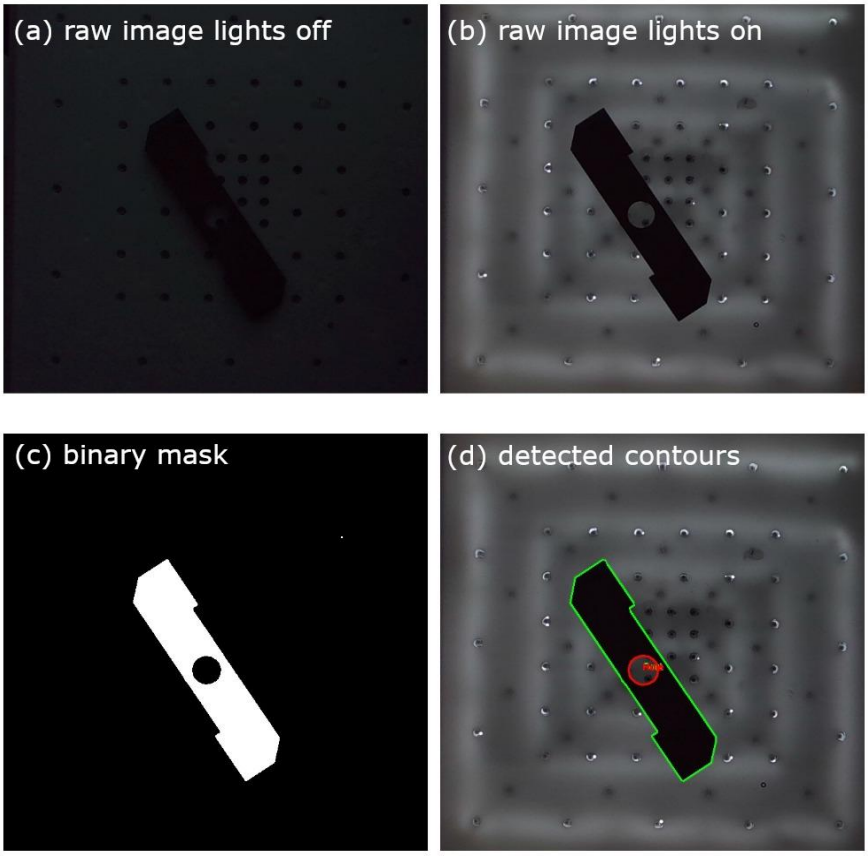

Fig. 4. Step-by-step images showing: (a) raw image, (b) background subtraction, (c) threshold, (d) detected contours

To transform detected image contours into robot coordinates, a robot–table calibration procedure was performed. The table surface was represented as a best-fit plane obtained from a semi-automated five-point probing routine. At each probing point, the robot approached the table using load-cell-based contact detection with a two-stage probing strategy consisting of a coarse contact and a slower fine contact. The resulting points were processed using singular value decomposition to determine the table plane and its orientation in the robot base frame. This calibration enabled the transformation of vision-detected features into robot coordinates with an estimated spatial accuracy of approximately ±2 mm.

Brushing was performed using a closed-loop proportional force control algorithm. During contour following, the robot continuously adjusted its vertical position to maintain a target normal contact force based on real-time measurements from the external load cell. This enabled compliant brushing despite local geometric variation and contour irregularities. Together, the integrated hardware setup, backlighting-based perception, calibration procedure, and force-controlled tool motion formed the experimental platform used to validate automated deburring of laser-cut sheet metal parts.

4. EXPERIMENTAL RESULTS AND PERFORMANCE ANALYSIS

The developed robotic deburring system was evaluated in terms of vision accuracy, force-control performance, deburring quality, and overall operational reliability. Across the experimental campaign, the integrated system demonstrated stable operation and produced repeatable deburring results on laser-cut sheet metal parts of different geometries. In total, 50 parts were processed, of which 48 were successfully detected, ground, and finished, corresponding to an overall success rate of approximately 96%. The failed cases were associated either with contour detection errors in the vision subsystem or with isolated brushing-process instabilities. The system successfully processed rectangular parts, hemispherical shapes, and more complex geometries containing holes larger than 6 mm, confirming that the approach is applicable to a moderate range of part types. At the same time, the experiments revealed practical operating limits, including reduced detection reliability for holes smaller than 6 mm and workspace restrictions caused by the robot singularity zone. Overall, the results indicate that the combined vision-guided and force-controlled brushing system provides a reliable basis for automated deburring of laser-cut sheet metal parts under controlled experimental conditions.

4.1. VISION SYSTEM PERFORMANCE

The performance of the vision system was assessed by comparing detected edge locations with the actual physical contours of the workpieces. The achieved spatial accuracy was approximately ±2 mm, which was considered sufficient for guiding the 25 mm abrasive brush used in the brushing process. This deviation corresponds to approximately 8 % of the tool diameter and therefore provides an acceptable tolerance for effective edge finishing without excessive material removal. The system successfully detected all tested external contours as well as internal features such as holes, although holes smaller than approximately 6 mm were not reliably identified because of the trade-off between noise suppression and small-feature sensitivity in the image-processing pipeline.

The theoretical imaging resolution of the camera setup was approximately 0.85 mm per pixel-equivalent detection limit, whereas the achieved practical accuracy was lower due to multiple sources of uncertainty, including reduced edge contrast, surface reflectance effects, image-processing artefacts, coordinate-transformation uncertainty, and calibration

inaccuracies. To improve robustness, the final system used optimized LED strip backlighting positioned below a translucent table surface, which produced a stable high-contrast silhouette of the workpieces. In addition, a dual-image background subtraction method was introduced to suppress false detections caused by the vacuum holding system, especially when vacuum nipples became covered with metal dust and visually resembled part edges. As shown in Fig. 5, this method significantly improved contour isolation compared with simple thresholding and was essential for reliable automated part localization.

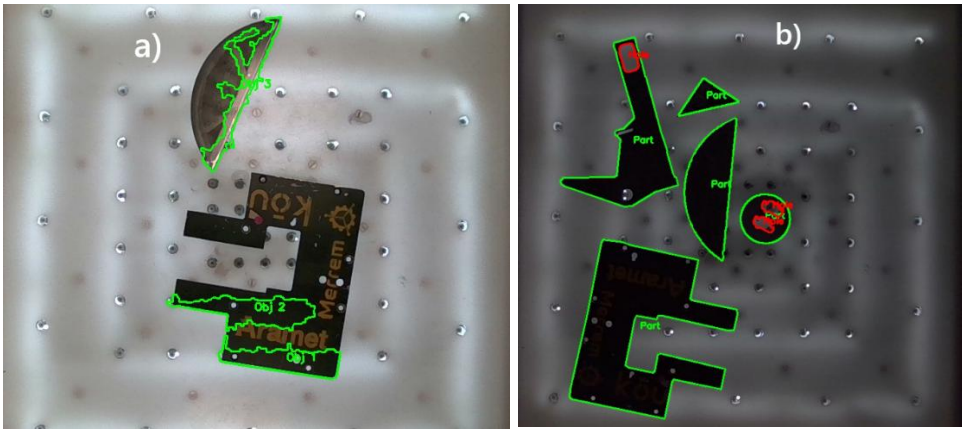

Fig. 5. Comparison images showing: (a) Failed detection with simple thresholding, (b) Successful detection with background subtraction

4.2. FORCE CONTROL PERFORMANCE

The force-controlled brushing system was evaluated at six feed rates between 5 and 30 mm/s for both external edge brushing and hole brushing, using a target contact force of ~12 N. The results showed very high force-tracking accuracy across all tested conditions. For part-edge brushing, the average achieved force was 11.68 N, corresponding to a mean deviation of −0.8 % from the target. For hole brushing, the average achieved force was 11.41 N, corresponding to a mean deviation of −3.1 %. The best tracking accuracy in both cases was achieved at 5 mm/s, while the largest deviations remained limited to −1.3 % for part brushing and −4.4 % for hole brushing. The overall force distributions, presented in Fig. 6, confirm that the controller remained well centred around the target value over the full range of tested feed rates.

Although mean force accuracy remained high, system stability decreased with increasing feed rate. As shown in Fig. 7 and Fig. 8, the variability of the contact force increased progressively at higher speeds. For part brushing, the standard deviation increased from 0.73 N at 5 mm/s to 1.82 N at 30 mm/s. For hole brushing, the corresponding increase was from 1.52 N to 3.47 N, indicating consistently higher variability for circular contours than for external edges. The detailed comparison is summarized in Table 1, which shows that hole brushing exhibited approximately 1.6× to 2.4× greater force variability than part brushing across the tested speeds. This difference can be attributed to the higher dynamic complexity of circular tool paths, which require continuous directional change and more demanding motion control.

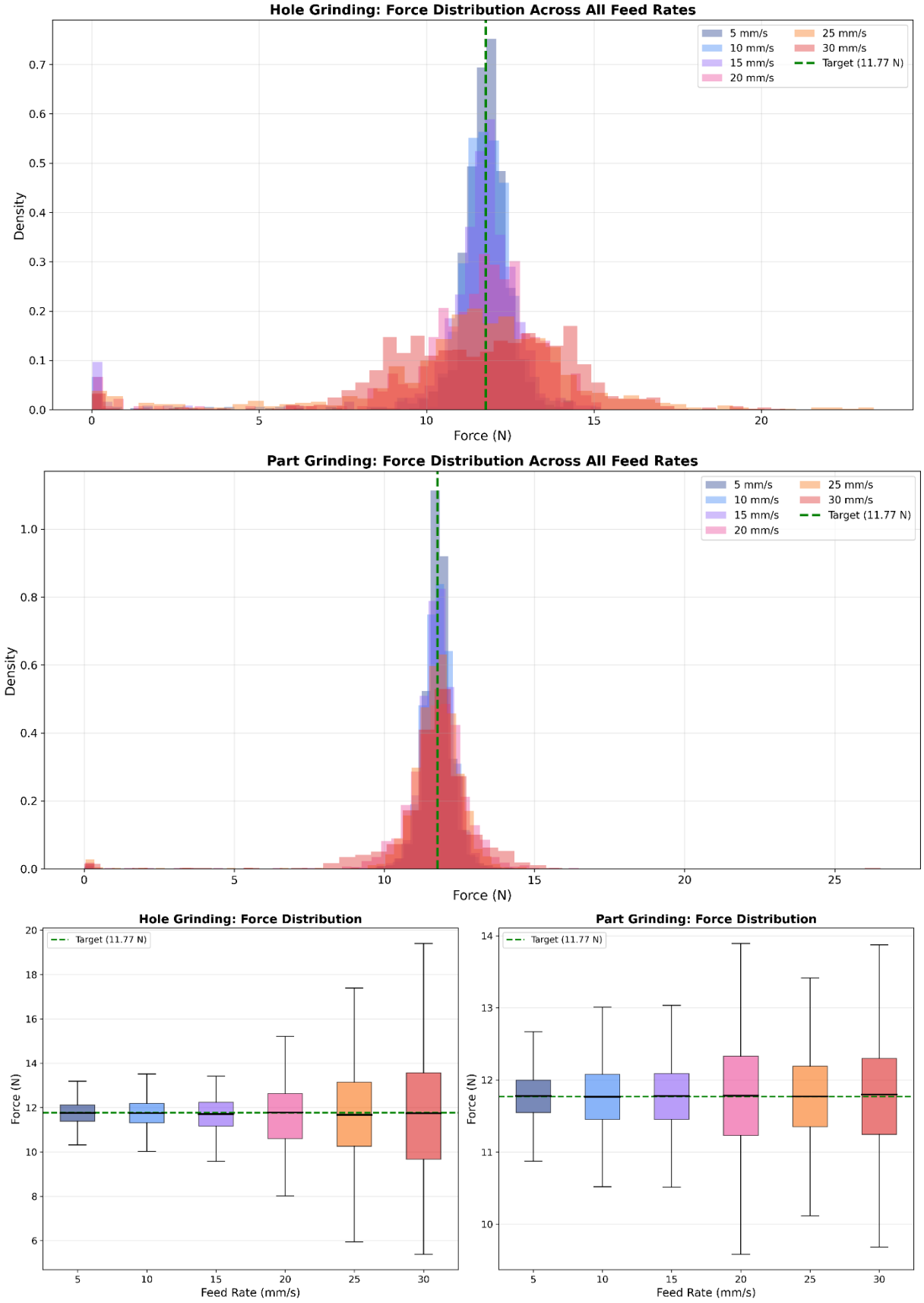

Fig. 6. Diagrams showing force distribution across all feed rates

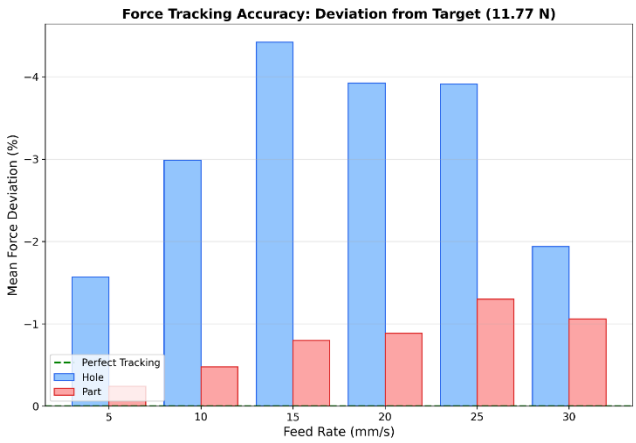

Fig. 7. Diagram showing force tracking accuracy deviation from target 11.77 N

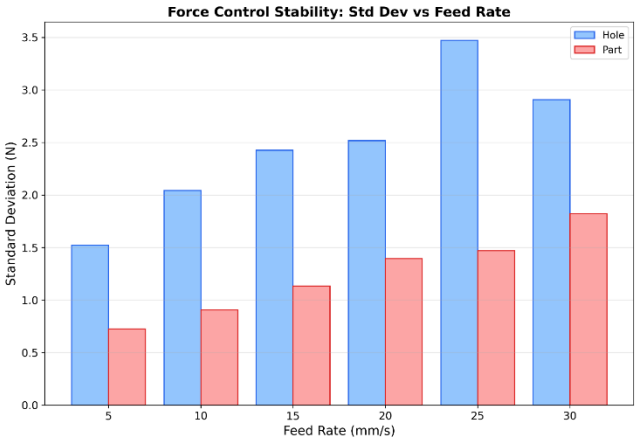

Fig. 8. Diagram showing force control stability (standard deviation) vs feed rate

Percentile analysis further showed that the median contact force remained close to the target value across all feed rates, indicating good calibration of the force-control loop. However, the increasing spread of the distributions at higher speeds suggests that excessive feed rates reduce process stability even when average force accuracy is preserved. Based on these results, the practical operating range for production-quality brushing was identified as 15–20 mm/s for part edges and 10–15 mm/s for holes. These recommended ranges provide a balance between force accuracy, stability, and cycle time. The main force-control results are summarized in Table 2, which highlights the average force levels, mean deviations from target, best achieved accuracy, and recommended feed-rate ranges for the two operation types.

Table 1. Detailed comparison of different speeds

Feed Rate	Part Std Dev	Hole Std Dev	Ratio (Hole/Part)
5 mm/s	0.73 N	1.52 N	2.1×
10 mm/s	0.90 N	2.04 N	2.3×
15 mm/s	1.14 N	2.42 N	2.1×
20 mm/s	1.39 N	2.52 N	1.8×
25 mm/s	1.47 N	3.47 N	2.4×
30 mm/s	1.82 N	2.90 N	1.6×

Table 2. Force Control Stability Summary

Metric	Part brushing	Hole brushing
Force	11.68 N	11.41 N
Mean deviation from target	-0.80%	-3.10%
Best accuracy (5 mm/s)	-0.30%	-1.60%
Optimal feed rate	15-20 mm/s	10-15 mm/s

4.3. BRUSHING QUALITY ASSESSMENT

Deburring effectiveness was evaluated primarily through qualitative inspection. The process was considered successful when the treated edge showed complete visible removal of burrs and dross, no detectable sharp edges in tactile inspection, and a visually uniform edge

surface after brushing. Thus, the present study evaluates process correctness in terms of practical edge-finishing quality rather than through quantitative surface roughness or edge-radius measurements. The results showed that the developed system successfully removed burrs, dross, and heat-affected edge defects in a single pass under the tested conditions. The system performed successfully on both mild steel and stainless-steel parts, and no significant difference in final brushing quality was observed between the two materials. Representative examples of edge improvement are presented in Fig. 9, which illustrates the before-and-after condition of processed parts.

Fig. 9. Before/after photos showing part quality improvement

In addition to finishing quality, the results also demonstrated promising overall robustness of the brushing process. Out of 50 processed parts, 48 were completed successfully, resulting in a success rate of approximately 96%. The isolated failures were linked to contour-detection limitations and local brushing-process instability rather than to fundamental shortcomings of the system concept. The process was validated on several geometry types, including rectangular plates, hemispherical parts, and complex contours with internal holes larger than 6 mm. However, several limitations remain: holes smaller than 6 mm were not reliably detected, the usable working area was limited by robot kinematics, and very thin materials below approximately 2 mm thickness were not included in the validation. Despite these constraints, the qualitative results confirm that the system can produce consistent and industrially relevant deburring quality on laser-cut sheet metal parts.

5. DISCUSSION

A limitation of the present work is that deburring quality was assessed qualitatively; future work should include quantitative metrics such as burr height reduction, edge radius, and surface roughness.

Although contour detection is a prerequisite for automated edge following, deburring effectiveness depends on additional process factors. In the present system, the final edge quality is determined by the interaction of contour localization accuracy, abrasive brush properties, contact force, spindle speed, and feed rate. The selected cylindrical abrasive brush and the validated force-control strategy enabled stable material removal under the tested conditions, but different brush types or parameter settings would be expected to influence burr removal efficiency, surface finish, and process stability.

6. CONCLUSION

This study presented an integrated robotic deburring system for laser-cut sheet metal parts that combines machine vision, robot–table calibration, and force-controlled brushing. The results show that the proposed approach can address the two key requirements of automated finishing: reliable localization of reflective parts and stable, compliant material removal.

The vision subsystem achieved a contour localization accuracy of approximately ±2 mm, which proved sufficient for guiding the 25 mm abrasive brush used in the experiments. Robust detection was enabled by the combination of a translucent inspection table, optimized LED backlighting, and a dual-exposure image-processing method. The system reliably detected external contours and larger internal features, although holes smaller than approximately 6 mm remained outside the reliable detection range.

The brushing experiments further showed that accurate robotic deburring requires external force sensing and closed-loop control. Mean force deviations remained below 1% for external edge brushing and below 4.5% for hole brushing, while the most stable operating range was identified as 15–20 mm/s for outer contours and 10–15 mm/s for holes. The results also confirmed that circular hole geometries produce higher force variability than external contours, emphasizing the importance of path geometry in robotic deburring performance.

In qualitative assessment, the system successfully removed burrs, dross, and heat-affected edge defects in a single pass for both mild steel and stainless-steel parts. Reliability testing yielded a 96% success rate, demonstrating stable system operation under the validated test conditions. At the same time, limitations were identified in the detection of very small features, the effective workspace, and process stability at higher feed rates.

Overall, the study confirms that vision-guided, force-controlled robotic deburring of laser-cut sheet metal is technically feasible and industrially relevant. The results provide a foundation for further development toward more robust and flexible automated finishing systems.

REFERENCES

[1] ONSTEIN I.F., SEMENIUTA O., BJERKENG M., 2020, *Deburring Using Robot Manipulators: a Review*, 3rd International Symposium on Small-scale Intelligent Manufacturing Systems (SIMS).

[2] BOGUE R., 2009, *Finishing Robots: a Review of Technologies and Applications*, Industrial robot, 36/1, 6–12, https://doi.org/10.1108/01439910910924611.

[3] NIKOLIC N., DJAPAN M., DAMJANOVIC A., RADENKOVIC M., 2022, *Implementation of Robotics for Lean Manufacturing Improvement*, International Journal for Quality Research, 1127–1140, https://doi.org/10.24874/ijqr17.04-10.
[4] ULLAH S., LI X., GUO G., 2022, *Influence of the Fiber Laser Cutting Parameters on the Mechanical Properties and Cut−Edge Microfeatures of a AA2B06−T4 Aluminum Alloy*, Optics & Laser Technology, 156.
[5] RAMARD M., LANIEL R., MIROIR M., KERBRAT O., 2025, *Quantification of the Influence of Morphologies on Laser Cutting Quality*, Journal of Machine Engineering, 25/1, 19–31, https://doi.org/10.36897/jme/203192.
[6] FALANDYS K., KURC K., BURGHARDT A., SZYBICKI D., 2023, *Automation of the Edge Deburring Process and Analysis of the Impact of Selected Parameters on Forces and Moments Induced During the Process*, Applied Sciences. 13(17):9646, https://doi.org/10.3390/app13179646.
[7] RAMSAUER C., OSWALD R., SCHÖRGHOFER P., 2022, *Primary Testing of an Instrumented Tool Holder for Brush Deburring of Milled Workpieces*, Journal of Machine Engineering, 22/2, 99–107, https://doi.org/10.36897/jme/149782.
[8] DOMROES F., KREWET C., KUHLENKOETTER B., 2013, *Application and Analysis of Force Control Strategies to Deburring and Grinding*, Modern Mechanical Engineering, 3/2A.
[9] ZHOU C., MENG M., 2023, *Research on a Method of Robot Grinding Force Tracking and Compensation Based on Deep Genetic Algorithm*, Machines, 1075.
[10] XUE X., HUANG H., 2022, *A Compliant Force Control Scheme for Industrial Robot Interactive Operation*, Front. Neurorobot, 16/2022.
[11] SELVARAJ T., LEO PRINCELY F., 2014, *Vision Assisted Robotic Deburring of Edge Burrs in Cast Parts*, Procedia Engineering, 1906–1914.
[12] MACMILLAN W.R., IRANI R.A., AHMADI M., 2023, *Planar Image-Space Trajectory Planning Algorithm for Contour Following in Robotic Machining*, CIRP Journal of Manufacturing Science and Technology, 42, 1–11.
[13] MAC MILLAN W., 2022, *Trajectory Planning for Contour Following*, Ontario: Ottawa-Carleton Institute for Mechanical and Aerospace Engineering.
[14] https://jlccnc.com/blog/cnc-deburring-tools-guide?utm_source=chatgpt.com.
[15] Eternal tools, 2024, What is Deburring: Your Guide to Removing the Rough Edges, https://eternaltools.com/blogs/tutorials/deburring-guide-to-removing-roughedges?srsltid=AfmBOorBtO_Np6rBiD-RGGw2KdyMempFjDoze2LgOWQR1c0y2Sm-GlCt&utm_source=chatgpt.com.
[16] XEBEC, 2026, https://www.xebec-tech.com/en/study/about_deburring/?utm_source=chatgpt.com.